Full Length Research Paper

Waste cooking oil transesterification: Influence of impeller type, temperature, speed and bottom clearance on FAME yield

Nabeel A. Adeyemi[1]*, Akm Mohiuddin[1] and Tariq Jameel[2]

[1]Department of Mechanical Engineering, International Islamic University
[2]Department of Biotechnology Engineering, International Islamic University Malaysia (IIUM),
Kuala Lumpur, Malaysia'

Waste cooking oil (WCO) provides an alternative source of raw material for biodiesel production. The reaction is both kinetics and mass transfer limited. Industrial use of current laboratory result suffer from dimensional non-compatibility because of the difference in the production environment especially as different impeller result in different flow characteristic during chemical reaction. In this work the effect of impeller type on fatty acid methyl ester (FAME) production from WCO was studied. At an alcohol oil mole ratio of 6:1 and 1% catalyst (oil weight), the Taguchi method was used for the experimental design of the transesterification in a 2 L stirred reactor using Rushton and elephant ear impellers. An optimum yield FAME at 70°C, 650 rpm impeller speed and 30 mm impeller bottom clearance (IBC) for Rushton impeller and 70°C, 700 rpm impeller speed and 25 mm IBC for an elephant ear impeller was obtained between 89 to 94%. IBC and speed were observed to have the most significant effect on yield using the signal to noise (S/N) ratio for Rushton and elephant ear impeller. Peak yield time between 5 to 30 min was observed. Correlation between FAME yield, peak time and temperature was high (0.968). The optimum reactor setting was at temperature 70°C, impeller speed of 650 rpm and IBC of 30 mm for Rushton (unbaffled reactor) and temperature 70°C, impeller speed of 700 rpm and IBC of 25 mm for elephant ear (baffled reactor). Physical configuration affected FAME yield/time in this work.

Key words: Waste cooking oil, transesterification, impeller, Taguchi, biodiesel.

INTRODUCTION

Alternative energy source like biodiesel (from fats/oils) using sustainable feed-stocks such as waste cooking oil (WCO) has become a main research concern due to the need to decrease focus on food oils as biodiesel raw material even as global vegetable oil production/consumption increases. Subsequently corresponding increase in industrial waste oil leads to disposal challenges (Zhang et al., 2003) which can be mitigated by using the waste oil as the production material for biodiesel. Apart from the environmental hazard of disposal, there are reports of adulteration of pure oils with low grade WCO (Catharino et al., 2005), which were hitherto discarded. Conversely with raw material representing 70% of the present biodiesel production cost (Demirbas, 2009), cheaper sources like non-food oils (de Sousa et al., 2010; Karmee and Chadha, 2005) and WCO (Araujo et al., 2010; Chhetri et al., 2008) are gaining wider attention as complimentary source of raw material for biodiesel production. Technically, biodiesel which are esters of fatty acid (most of which are fatty acid methyl ester, FAME) is produced from oils using straight chain alcohol. Numerous studies have been carried out on FAME production from various oils with focus on oil type (Sharma et al., 2008), temperature of reaction (Ma et al., 1998), types of catalyst (Freedman et al., 1986; Jena et al., 2010) Baroutian et al., 2010; ratio of alcohol

---

*Corresponding author. E-mail: adeyemi.nabeel@student.iium.edu.my,nabadeyemi@yahoo.com. Tel: +60182478335.

to WCO (Valle et al., 2010; Zhou and Boocock, 2006), free fatty acid and moisture content (Knothe and Steidley, 2009; Kulkarni and Dalai, 2006; Meher et al., 2006). These afore-mentioned factors are viewed as critical aspect of the biodiesel production. At a stoichiometric ratio of 3:1 (alcohol to oil), the conversion of oil to FAME takes place in the presence of a homogenous catalyst.

The reaction mechanism is understood to be the formation of two intermediates (Meher et al., 2006) before forming the final product or the formation of only one intermediate subsequent to formation of the products (Freedman et al., 1986). Transesterification process is benefited by the low moisture content (0.1%) and free fatty acid (FFA) (<5%) (May, 2004). The biodiesel produced from WCO compares favorably with biodiesel from neat oil with respect to oxidative stability (Ramos et al., 2009), acid and iodine value (Mittelbach and Schober, 2003; Vicente et al., 2004). Excellent reviews on biodiesel production (Gui et al., 2008; Knothe and Steidley, 2009; Kulkarni and Dalai, 2006) highlight these conditions in detail for various oil types. FAME production employs mixing impellers to promote characteristic multiphase mixing (Yang et al., 2008) and the hydro-dynamic feature such as mixing time and resident time within the reactor determines FAME quality. Stamenkovic et al. (2007) highlighted that chemical reaction kinetics are affected by physical environment of the reactor and hydrodynamic studies has been used to understand the effects created by reactor configuration in single/ multi-phase reactive flow (Szalai et al., 2003) in stirred environment. Meher et al. (2004) conducted trans-esterification reaction with 180, 360 and 600 revolutions per minute (rpm) and reported incomplete reaction at 180 rpm but the yield of methyl ester was same at 360 and 600 rpm. In a previous work by same author, the yield of biodiesel increased from 85 to 89.5% when magnetic stirrer (1000 rpm) was replaced with mechanical stirrer (1100 rpm). In other studies (Bautista et al., 2009; Ferella et al., 2010) where WCO served as raw material and based on the catalyst concentration, temperature and reaction time at mixing speed between 600 to 700 rpm, the effect of catalyst and FFA were found to be significant on FAME purity with temperature having a more significant effect on yield than purity without any recourse to the effect of stirring.

The industrial application of such laboratory result suffers from dimensional non-compatibility (Fernandes, 2010) during scale up even though procedure used for industrial production of biodiesel is very similar to that used on a laboratory scale. Fluid flow in a mixing vessel is primarily a function of the fluid rheology, tank geometry, and the design and operation of the impellers, invariably determining mix quality. Based on the interrelationship of reaction and mixing, very few works are reported with regards to mixing for FAME production from WCO in stirred tanks even though the importance is implied in some of the detailed kinetic studies of palm oil transesterification (Darnoko and Cheryan, 2000; Noureddini

and Zhu, 1997). The relevance of the mixing effect will be very important in improving the biodiesel production in stirred reactor. The objective of this study was to establish the effect of reactor parameters such as type of impeller, baffle, IBC configuration and temperature on FAME production in a stirred batch reactor considering that the reaction time affects product quality and quantity. It is expected that this knowledge would improve yield during laboratory studies for subsequent industrial application.

MATERIALS AND METHODS

WCO samples and chemical

WCO samples were collected from local food malls between the periods of January 2009 to December 2009. Reference standards of FAMEs for the analysis were 100 mg neat mixture, containing C16:0, C18:0, C18:1 and C18:2 FAMEs (2 to 4% relative concentrations = 0.2 to 0.4 mg/ml per FAME) supplied by Supelco, Malaysia. Methanol (95%), sodium hydroxide pellets, GC MS biodiesel (MSTFA derivatization kit, 10 x 1 ml ampoule) kit containing glycerin, monoolein, diolein, triolein (ASTM D6548 solutions), butanetriol and tricaprin (internal standard #1 and 2#, 44918 U) at concentrations specified according to ASTM D6584/6751 were supplied by Sigma Aldrich, Malaysia. These were used to quantify the triglyceride (T), diglycerides (DG), monoglyceride (MG) and free glycerin (G). Laboratory grade potassium hydroxide (KOH), isopropyl alcohol and phenolphthalein were used for the FFA estimation.

Transesterification of WCO

Sodium hydroxide (NaOH) catalyst (1.5% by wt) was dissolved in the methanol (140 cm^3). A stoichiometric molar ratio of 1:6 (oil: alcohol) was used. Although a theoretical ratio of 1:3 is needed for the reaction, excess methanol was needed in other to drive the reaction forward. These parameters were kept constant while other physical parameters of the reactor (Table 1) were varied according to the experimental design. All mixing were carried out for 60 min.

Physical dimension of reactor

The physical dimension of the 2 L desktop laboratory reactor used is shown in Table 1. A variable speed motor, automatic timer and temperature controller were connected to the reactor as speed and temperature controllers. A reflux condenser was fitted over the reactor for methanol reused. The impellers used were standard Rushton and elephant ear impellers supplied along with the 2 L table top laboratory glass reactor.

Evaluation of FFA in WCO

For the evaluation of the FFA in WCO sample, 50 cm^3 isopropyl alcohol was prepared and added to 1 g of WCO sample in the presence of 1 g phenolphthalein. The solution was titrated against 0.1 M KOH until color change was noticed in the solution. This was done in triplicates and the average FFA was calculated by Equation 1:

$$\frac{25.6 \times 0.0864 \times difference\ in\ \mathrm{NaOH}\ volume}{sample\ weight} = FFA\%\quad(1)$$

Table 1. Reactor dimension.

Parameter	Dimension (mm)
Height (H)	150
Tank diameter (T)	65
Total liquid height (L)	48
Rushton-impeller diameter (D)	50
Impeller blade height	12
Elephant ear-impeller diameter (D)	55
Impeller blade height	45

Table 2. Taguchi design variables.

Variable	Level		
	1	2	3
Temperature (T, °C)	60	65	70
Impeller speed (S, rpm)	600	650	700
Impeller bottom clearance (IBC, mm)	20	25	30

Taguchi method design of the experiment

The experiment was based on the Taguchi orthogonal array (OA) L_9 method (Paul et al., 2004). Three variables (temperature, speed and IBC) at three levels were used to design the experiment (Table 2) in MINITAB 14. Taguchi method based on OA reduces variance for the experiment with optimum setting of the control parameters. To identify the combined effect of temperature, impeller speed and IBC on yield, the S/N ratio of the Taguchi method, (which is log functions of desired output) was used for data analysis and prediction of optimum parameters. The signal noise (S/N) is defined as:

$$\frac{S}{N_{(Bigger)}} = -10\log\left[\frac{\sum\left(\frac{1}{y_1^2}\right)}{n}\right] \qquad (2)$$

Where, n is the number of observations in the sub-sample and y is the data observations in the subset.

The S/N is used to calculate the performance statistics values and contribution ratios of each parameter. Thus the combination of design of experiments with optimization of control parameters to obtain best results is achieved in the Taguchi method. OA provides a set of well balanced (minimum) experiments. Without the Taguchi method, 16 experiments would have been needed to investigate the effects of each of the three parameters instead of the nine used. The S/N ratio of the results is used to analyze the yield. With the main effect analysis, possible combination of optimum parameters is predicted. These were further analyzed to determine the interactive effect of the three parameters for a dynamic model.

Standards and sample preparation for T, DG, MG and glycerol analysis

GC MS analysis of biodiesel according to ASTM D6584 was used to verify the free glycerin (G), mono-glycerides (MG), diglycerides (DG), tri-glycerides (T), and total glycerin (TG) content in WCO and FAME samples. Experimental samples were analyzed on a Agilent 7890 A Series GC with cool-on-column inlet with electronic pneumatics control (EPC) (McCurry et al., 2007). 5 GC calibration standards were prepared by mixing aliquots of the individual stock standards in proportions specified by the ASTM method. After mixing, 100 µl of the derivatization agent, N-Methyl-N-(trimethylsilyl) trifluoroacetamide (MSTFA) was added to each calibration standard. After 20 min, 8 ml of reagent grade n-heptanes was added to each calibration standard. These final reaction mixtures were directly injected into the gas chromatograph (McCurry et al., 2007).

Sample preparation for fatty acid analysis

Reference standards of FAMEs were a mixture, purchased as a 100 mg neat mixture, containing C4 to C24 FAMEs (2 to 4% relative concentration) for the analysis. The reference standards were dissolved in hexane at a 0.01 to 0.1% (w/v) concentration. The whole sample was diluted in 10 ml of hexane (final concentration = 0.2 to 0.4 mg/ml per FAME). WCO samples were analyzed by weighing 100 mg sample in a 20 cm^3 test tube (with screw cap) and dissolved in 10 cm^3 of hexane. 100 µl of 2 M KOH in methanol (11.2 g in 100 cm^3) was added and vortex for 30 s. The supernatant was then transferred into a 2 cm^3 auto sampler vial for GC analysis. DB 23 Agilent 6890 GC system with a split/splitless inlet and a column of 60 m × 0.25 mm id × 0.15 µm was used for the FAME analysis (David et al., 2002).

GC MS analysis of T, DG, MG and glycerol

FAME yield was obtained by Equation 3 during the reactions at time intervals of 5, 10, 15, 30, 45 and 60 min. T, DG, MG and glycerol content in the FAME samples were estimated using the relative retention times from the GC reading (McCurry et al., 2007). The retention time of the first internal standard, 1,2,4-butanetriol was used to identify and quantify free glycerin (G) while that of the second internal standard, tricaprin, was used to identify and quantify the MGs, DGs, and Ts in the monoolein, diolein, and

Table 3. Composition of fatty acids and glycerides in WCO samples.

Component	Amount
C16:0 (%)	37.05
C18:0 (%)	10.54
C18:1 (%)	46.21
C18:2 (%)	4.820
T (mol/L)	0.497
DG (mol/L)	0.822
MG (mol/L)	0.0891
Glycerol (mol/L)	0.0137

triolein calibration functions, respectively. Total glycerin (TG) was obtained using Equation 4:

$$\text{Yield (wt \%)} = \frac{m_{ester}}{3 \times m_{oil}/MW_{oil} \times MW_{ester}} \times 100 \quad (3)$$

Where M_{ester} = mass of ester, MW_{ester} = molecular mass of ester, MW_{oil} = molecular mass of oil, M_{oil} = mass of oil:

$$TG = G + 0.255M + 0.146D + 0.103T \quad (4)$$

Average composition of fatty acid, T, DG, MG and G from GC-MS data for WCO is shown in Table 3. The T, DG, MG and G of the FAME were mostly within the ASTM specification for B100 biodiesel (Table 4). Densities of samples were measured using a KVS 702 tensiometer at room temperature. WCO and FAME density averaged 909 and 847 g/m³ respectively and molecular weight of the WCO samples ranged between 864 to 894.4 g/mol. FFA of the WCO samples varied from 0.67 to 3.98 mg KOH/g, that is, < 2%. This was quite low contrary to expectation because used oil had been reported to contain high FFA (Canakci, 2007). High FFA result in saponification during WCO transesterification, necessitating acid transesterification to reduce the FFA level (Berrios et al., 2007). According to Knothe and Steidley (2009), used oil could exhibit varying acid, FFA and oxidation values as a result of conditions under which they were used. This low level of FFA in the WCO samples could be advantageous for an alkali catalyzed transesterification process using WCO from local food vendors in Malaysia.

RESULTS AND DISCUSSION

In this work FAME yield as a result of the impeller speed, IBC and temperature was compared and analyzed at first without consideration of the period of maximum yield. The reaction condition with regards to the molar ratio of oil to alcohol and catalyst amount was according to the optimized value used for fryer grease transesterification (Issariyakul et al., 2007).

Effect of impeller type, position and speed on yield: Rushton impeller

The ester yields from the transesterification reaction at three different impeller clearances of 20, 25 and 30 mm

carried out were as shown in Figures 1 and 2 using a Rushton impeller in baffled and unbaffled reactor. In Figures 1a to c, the 20 mm IBC for the Rushton at all the temperatures resulted in the highest FAME yield (91 to 92%) at 600 rpm. At 60°C, the highest FAME yield was observed at 650 rpm for 25 and 30 mm IBC, while a decreasing trend was noted at 20 mm IBC (Figure 1a). A significant reduction was however noticed at 650 rpm for 30 mm IBC. At 70°C (Figure 1c), the converse was observed where the highest FAME yield was noted at 650 rpm for both 25 and 30 mm IBC and the highest yield at 600 rpm for 20 mm IBC. The entire FAME yields were between 91 to 92%. However a clear cut trend for FAME yield was not identified as a result of the different speed and IBC. For the unbaffled reactor at 60°C (Figure 2a), peak FAME yield was recorded at 650 rpm for all the IBC however the yield at 700 rpm was not significantly different. At 65°C, the trend was somewhat different. FAME yield was significantly different at all the speed and it increased steadily for the 25 mm IBC (Figure 2b) for all the speed. The yield at 70°C (Figure 2c) indicated also an increasing pattern from 650 to 700 rpm at 25 and 30 mm IBC.

From the aforementioned, 20 mm IBC for the Rushton at all the temperatures resulted in a higher FAME yield at 600 rpm compared to speed at 650 and 700 rpm in the baffled reactor, while the highest yield (91 to 92.5%) was found at 650 rpm in the unbaffled reactor for the 20 and 25 mm IBC. The exception was the 93% yield for 700 rpm at 25 mm in the unbaffled reactor.

Effect of impeller type, position and speed on yield: Elephant ear impeller

Incremental yield was recorded with increase in speed at 25 mm IBC in the unbaffled reactor for all the speed (88.6 to 92%) representing 16, 15 and 2% increase in yield at 60°C for the three speeds. There was no significant difference between the yield at 600 and 700 rpm for the 20 and 30 mm IBC, with the lowest yield (86%) at 70°C (Figure 3c). In the unbaffled reactor, the highest yield was obtained at 60°C (Figure 4a) for 650 rpm (89.5 to 91%). However, at 65°C (Figure 4b), yield decreased by 5% at 650 rpm as compared to the 600 and 700 rpm but the yield was not significantly different at other speeds. An overall assessment of the yield at 60°C for the unbaffled reactor with Elephant ear shows the highest yield at 650 rpm for 20 mm IBC. Similarly yield increased with speed 600 to 650 rpm for 25 mm IBC. At 70°C (Figure 4c), the FAME yield was observed to increase steadily for 20 and 25 mm IBC from 600 to 650 rpm. However, the yield at 600 rpm for 25 mm IBC was the lowest compared to the other speeds. Overall, FAME yield was between 86 to 93%. Table 5 shows the mean FAME yield at different temperature and speed. For the Rushton impeller, the magnitude of error was lowest (0.21, 0.37 and 0.07) at 60°C and 650 rpm; 65°C and 650 rpm and 70°C and 600

Table 4. WCO FAME compared to ASTM D6584 standard.

Parameter	ASTM standard	Rushton (unbaffled)	Rushton (baffled)	Elephant ear (unbaffled)	Elephant ear (baffled)
MG	0.800 %(m/m)	0.0495	0.0405	0.057	0.049
DG	0.200% (m/m)	1.713	1.312	0.590	0.425
T	0.200% (m/m)	0.490	0.394	0.591	0.489
G	0.020% (m/m)	0.019	0.015	0.021	0.281
TG	0.250%(m/m)	0.331	0.256	0.181	0.404
Density at room temperature (g/cm³)	0.860-0.910	0.847	0.846	0.849	0.849
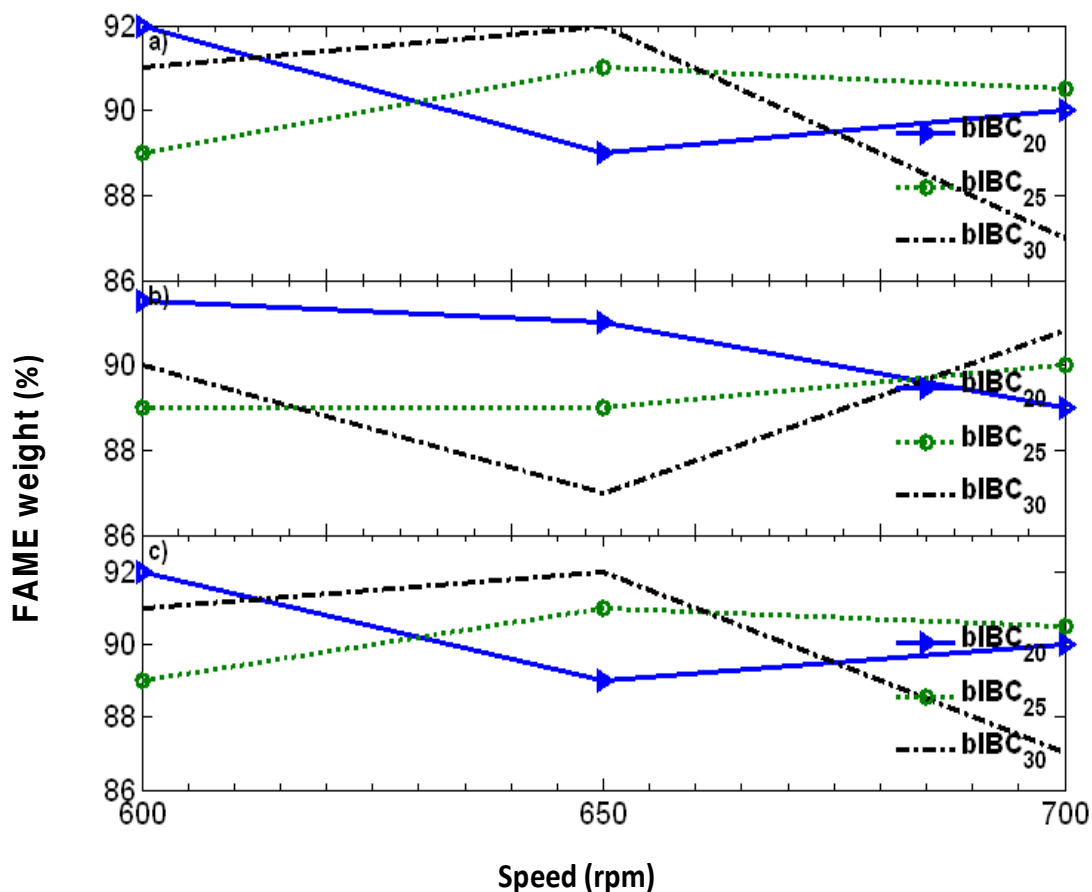
Figure 1. FAME weight (%) at (a) 60, (b) 65, (c) 70; C for N = 600, 650, 700 rpm and IBC = 20, 25, 30 mm for Rushton impeller in baffled reactor.

rpm in the unbaffled reactor respectively, while the lowest error was found for the baffled reactor for 60°C at 600 rpm; 65°C at 600 rpm and 70°C at 650 rpm. With the Elephant ear, the magnitude of error was lowest at 700 rpm for 60°C; 650 rpm for 65°C and 600 rpm for 70°C for the unbaffled reactor, while that of the baffled system was 0.43, 0.58 and 0.35 at 700 rpm for 60°C, 650 rpm for 65°C and 600 rpm for 70°C respectively.

The results partly indicate that higher yield was obtained in the Rushton unbaffled reactor (92.4%) at 650

rpm and 60°C on the average compared to the highest yield using the Elephant ear which gave 91.17% at 700 rpm and 65°C. Further analysis of this data was needed to confirm the effect of the impellers on FAME yield. Although the effect of IBC, speed and baffle with the two impellers on yield was noted, but the confirmation of the particular parameter to be optimized was needed. The mean yield in the design was used as criterion to select the parameter for design. Here the Rushton (unbaffled) resulted in the highest (92.43%) yield at 650 rpm and the
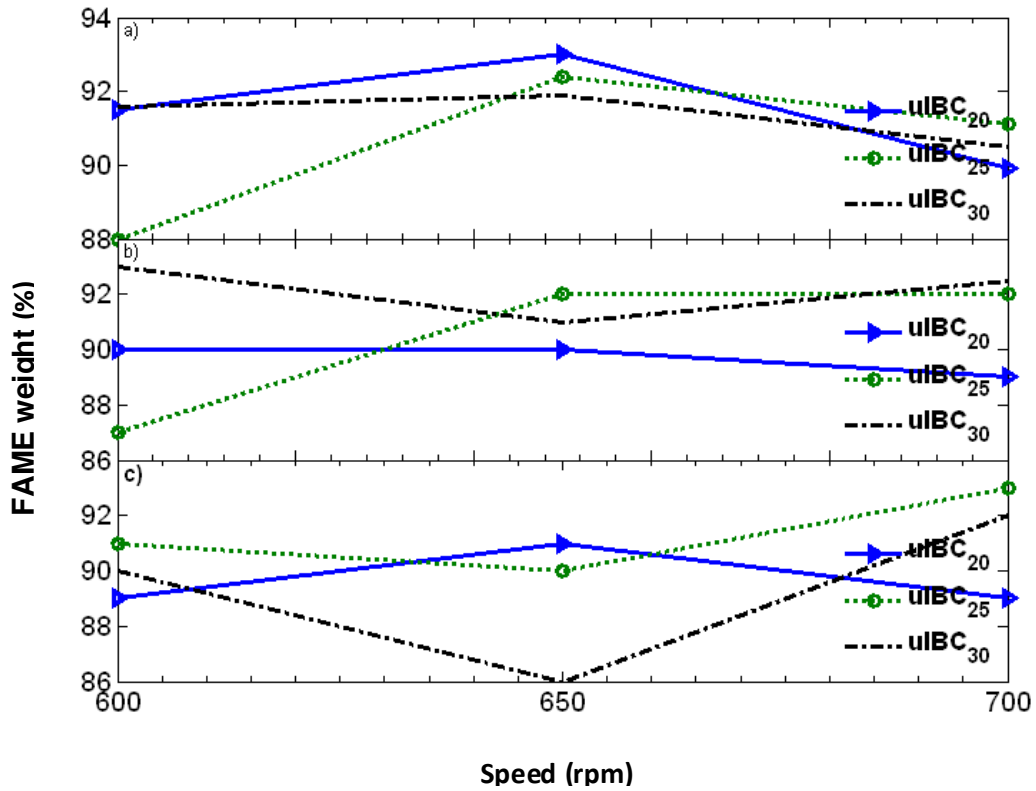
Figure 2. FAME weight (%) at (a) 60, (b) 65, (c) 70; C for N = 600, 650, 700 rpm and IBC = 20, 25, 30 mm for Rushton impeller in unbaffled reactor.
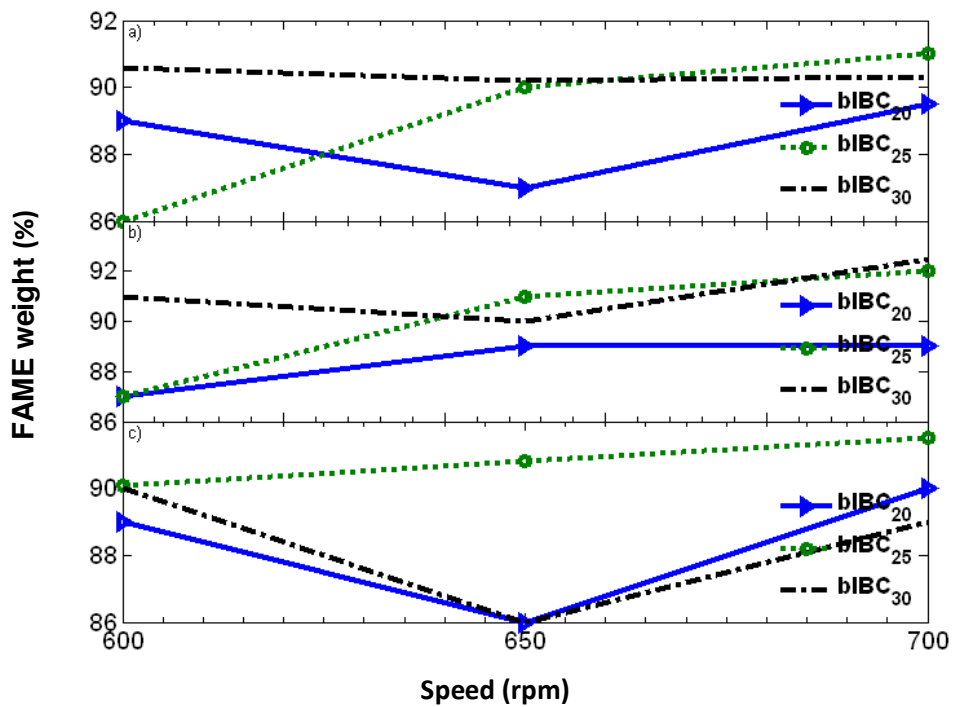
Figure 3. FAME weight (%) at (a) 60, (b) 65, (c) 7; C for N = 600, 650, 700 rpm and IBC = 20, 25, 30 mm for Elephant Ear impeller in baffled reactor.
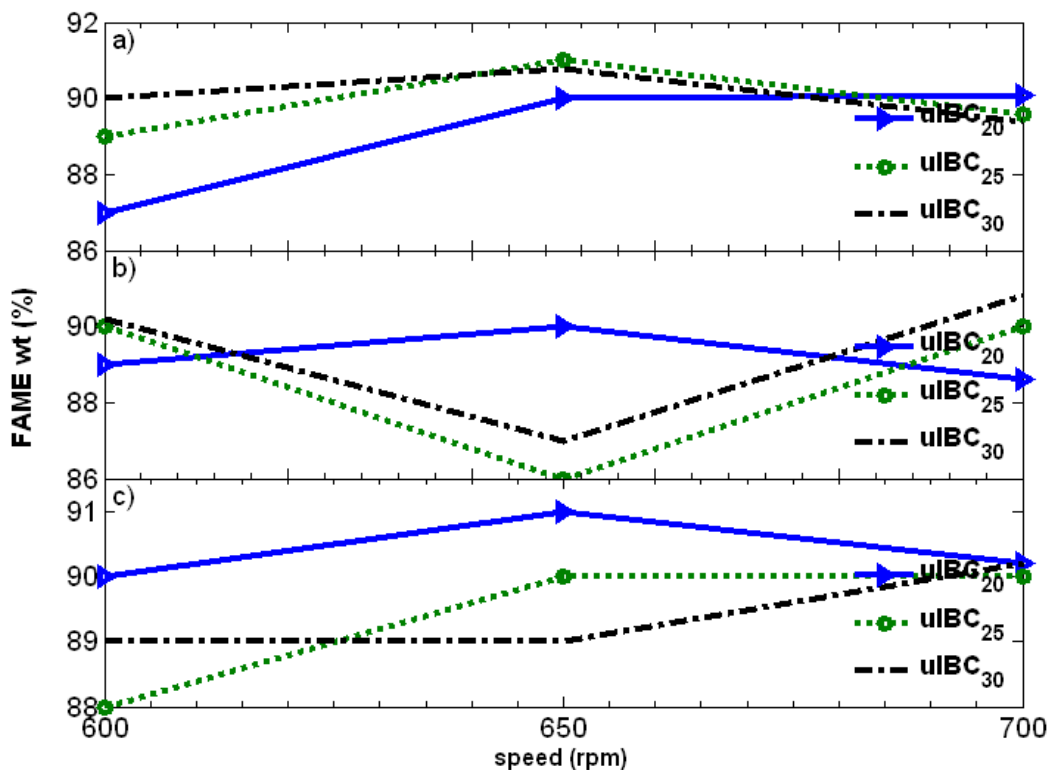
Figure 4. FAME weight (%) at (a) 60, (b) 65, (c) 70, C for N = 600, 650, 700 rpm and IBC = 20, 25, 30 mm for Elephant Ear impeller in unbaffled reactor.

Elephant ear (baffled) at 700 rpm (91.17%). Hence the design of the experiment was based on these two conditions. This was carried out by obtaining the FAME concentration at the stated time interval and the result was used to analyze the effect of the three parameters on the FAME yield during the reaction. It should be noted that unlike the earlier investigations (Chhetri, 2008 #1714) and (Bautista, 2009 #1327) peak yield time was added in our consideration and analysis. Table 2 shows the experiment design. The result of the L_9 design was discussed. It was observed that, FAME yield increased with increasing agitation speed in the 2 L reactor for 30 min of the reaction duration. The FAME yield at 600 rpm was in the order of 70→60→65°C and the reaction peaked at 30 min as compared with the reaction at other temperatures (Figure 5a). The trend at 650 rpm and 700 rpm (Figures 5b and c) was in the order of 60→70→65°C. The effect of IBC on yield was also obvious as shown in Figures 6a, b and c. At 20 mm IBC, in terms of conversion, the yield order was 60→70→65°C (Figure 6a). The highest yield was seen at 15 min reaction time. For the impeller position at 25 mm (Figure 6b), the yield order was 70→60→65°C. Also the peak conversions noticed were at 5 and 15 min.

At a 30 mm IBC, the yield peaked at 15 min mark and the conversion followed a 60→70→65°C order. The highest yield was recorded at 15 min.

Effect of impeller type, position and speed on yield: Elephant ear impeller

Figures 7a, b and c show the distribution of the FAME produced at 600, 650 and 700 rpm respectively. The FAME yield at 600 rpm was in the order of 60→65→70°C and the reaction peaked at 5 and 15 min (Figure 7a) as compared with the reaction at other temperatures. At 650 rpm, the trend of yield was in the order from 65→70→60°C (Figure 7b). At 700 rpm, this trend was 60→70→65°C where the peak FAME yield was observed at the 10 min (Figure 7c). The effect of IBC on yield was also obvious as shown in Figures 8a, b and c. At 20 mm IBC, in terms of the yield, the order was 60→65→70°C (Figure 8a). For the impeller position at 25 mm IBC (Figure 8b), the highest conversion was seen at 5 min in the order of 65→70→60°C. At 30 mm IBC (Figure 8c), the peak yield was between 5 to 10 min in the order of 65→60→70°C. Two yield peaks were noted at 20 and 30 mm IBC (Figure 5c) at 700 rpm. The flow pattern using a Rushton impeller creates a flow loop when fully immersed in a fluid. At these distances, the impeller is either immersed with a large IBC (that is 30 mm) that would require greater recirculation period between the fluids been mixed. It was noticed that two yield peaks were recorded using Rushton Impeller. This could be attributed to delayed contact between the WCO and alcohol in the

Table 5. Mean FAME yield, standard deviation and error for baffled and unbaffled reactor with Rushton and Elephant Ear impeller.

Impeller type	FAME yield	Temperature (°C)								
		60			65			70		
		Speed (rpm)								
		600	650	700	600	650	700	600	650	700
Rushton Unbaffled	Mean yield (%)	90.37	92.43	90.50	90.02	91.01	91.17	90.01	89.03	91.33
	Standard deviation	2.05	0.55	0.60	3.0	1.0	1.89	1.0	2.65	2.08
	Error	1.18	0.32	0.35	1.73	0.58	1.093	0.58	1.53	1.20
Rushton Baffled	Mean yield (%)	90.67	90.67	89.17	90.17	89.00	89.93	89.00	89.53	90.00
	Standard deviation	1.53	1.53	1.89	1.26	2.00	0.90	2.65	0.50	1.00
	Error	0.88	0.88	1.09	0.73	1.15	0.52	1.53	0.29	0.58
Elephant Ear Unbaffled	Mean yield (%)	88.67	90.6	89.7	89.73	87.67	89.8	89.00	90.00	90.13
	Standard deviation	1.53	0.53	0.36	0.64	2.082	1.11	1.00	1.00	0.12
	Error	0.88	0.31	0.21	0.37	1.20	0.64	0.58	0.58	0.07
Elephant Ear Baffled	Mean yield (%)	88.53	89.07	90.27	88.33	90	91.17	89.7	87.6	90.17
	Standard deviation	2.34	1.79	0.75	2.31	1	1.89	0.61	2.77	1.26
	Error	1.35	1.03	0.43	1.33	0.58	1.09	0.35	1.6	0.73
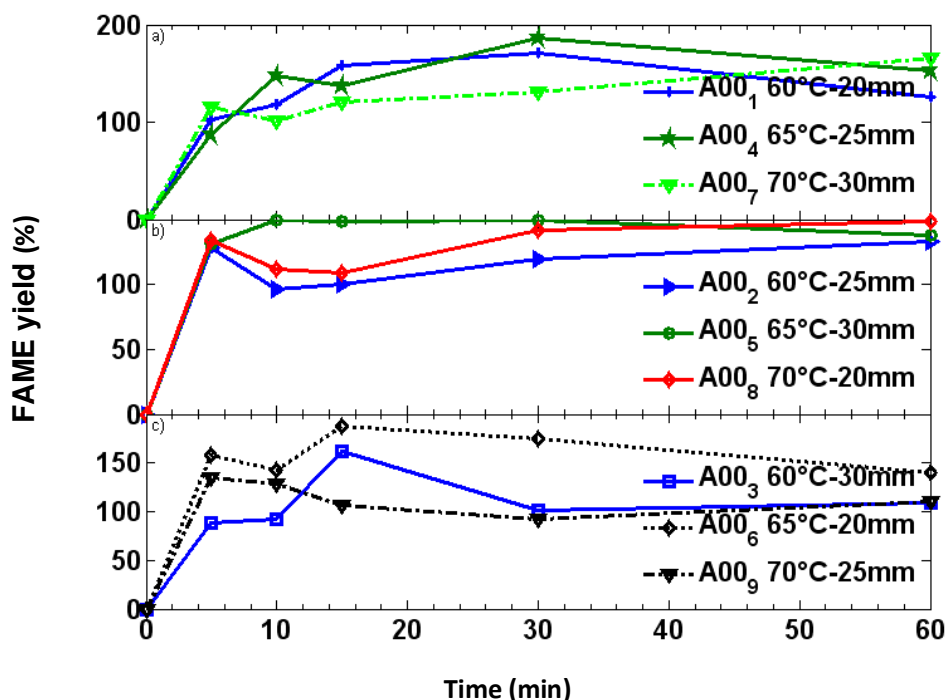
Figure 5. FAME plot for Rushton impeller (baffled) at impeller speed (a) 600rpm, (b) 650rpm, (c) 700rpm.

unbaffled reactor. At 20 mm IBC, a near solid body motion of the fluid was also observed which necessitated a longer mixing period for full phase contact. However, the reduction in speed (Figure 5a) resulted in an
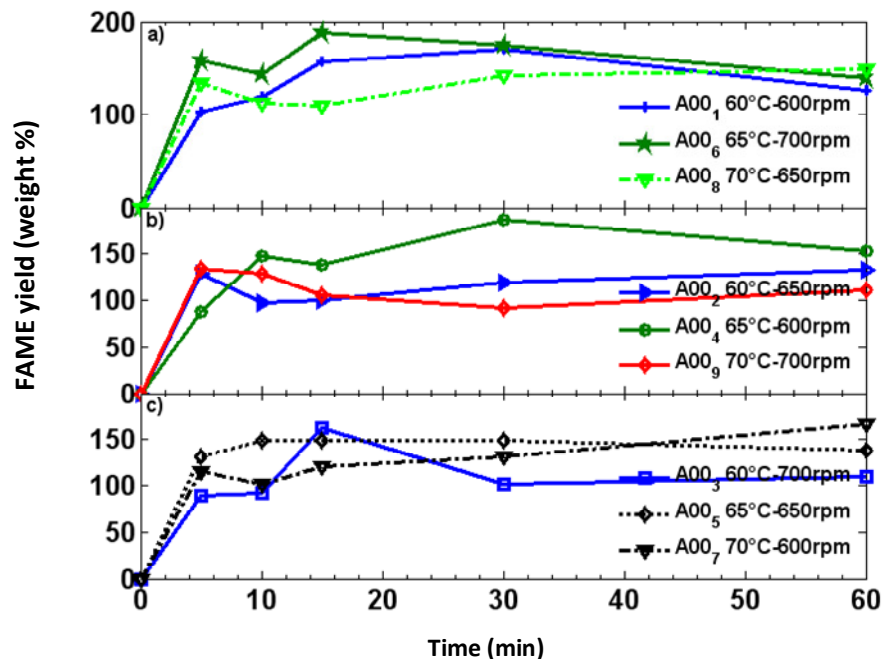
Figure 6. FAME yield for Rushton impeller (unbaffled) at IBC of (a) 20 mm, (b) 25mm and (c) 30mm.
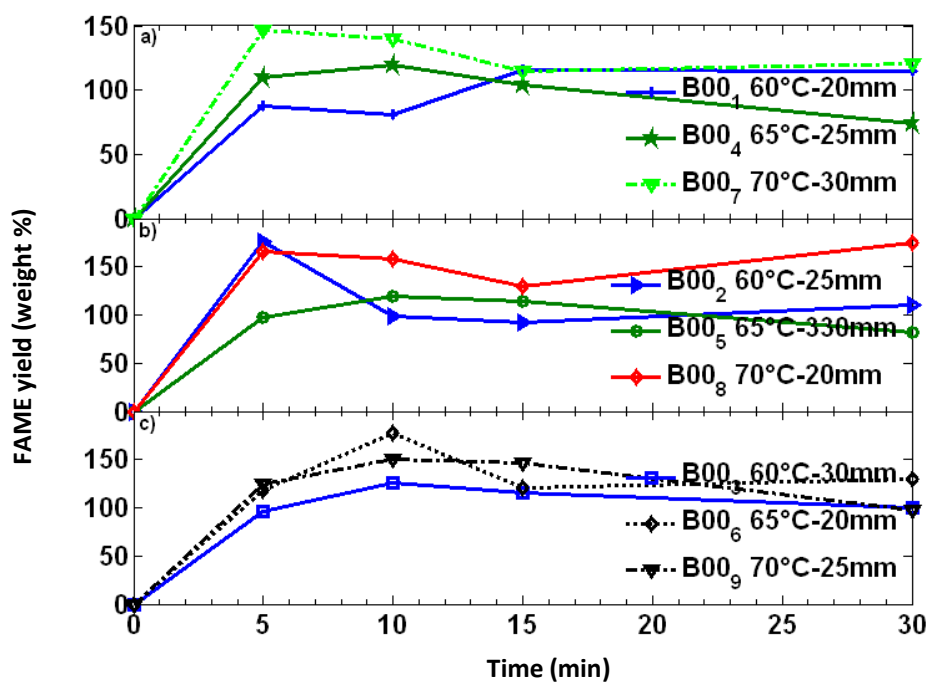
Figure 7. FAME plot for Elephant ear Impeller (baffled) at Impeller speed. (a) 600 rpm; (b) 650 rpm; (c) 700 rpm.

exponential-like increment in the FAME concentration at all the IBC. Alternately, for the case where the elephant ear impeller was also accompanied with a baffle, peak yield were recorded in the first 5 to10 min. The baffles

themselves assisted in preventing swirling without interfering with radial and longitudinal flow.

Low viscosity liquid mixing is affected by strong current and destroys stagnant pockets once swirling stops the
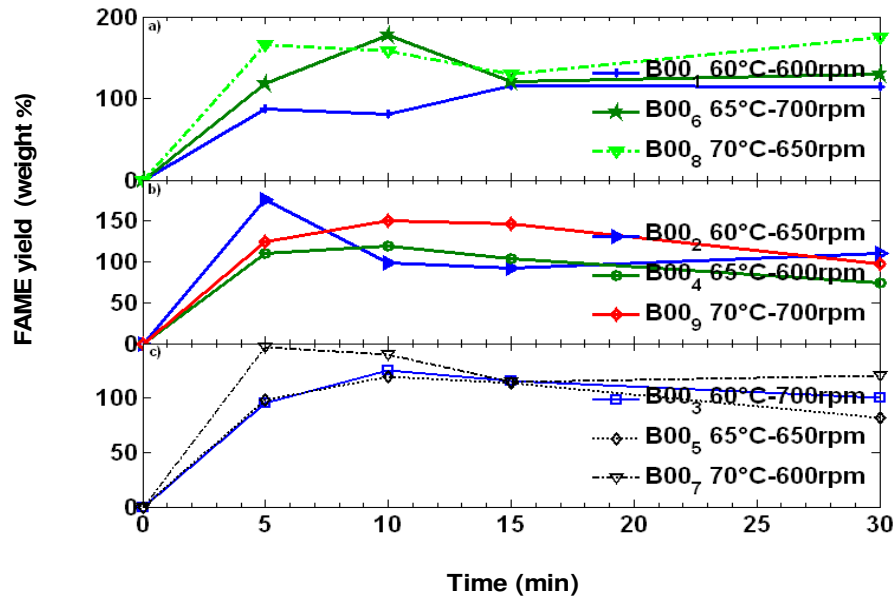
Figure 8. FAME plot for Elephant ear (baffled) at Impeller speed (a) 20 mm, (b) 25 mm and (c) 30 mm.

flow pattern which depends on the type of impeller. The Rushton impeller is noted for a jet-like dispersion from the tip and the depth of immersion (that is bottom distance); determines the extent of dispersion and quality of flow generated by the impeller.

Statistical analysis response of L$_9$ Taguchi design of the experiment

Using the maximizing function (largest is best) of the Taguchi method (Equation 2), the analysis of the experimental design is shown in Table 5. From the statistical analysis, the ranking of the factors on yield in order of importance was as follows:

Rushton: IBC → temperature → speed.
Elephant ear: speed → IBC → temperature.

From Table 6, for the Rushton impeller, the highest S/N ratio obtained was at temperature 70°C, speed 600 rpm and IBC of 30 mm. Similarly, the highest S/N ratio for the elephant ear was obtained at temperature 60°C, speed 650 rpm and IBC of 25 mm. The factor level was thus adjusted and chosen for design optimization. Adjusting the factor level, an S/N ratio of 39.25 was predicted at temperature 70°C, speed 600 rpm and IBC of 30 mm for the Rushton impeller. Similarly, S/N ratio for the elephant ear at temperature 60°C, speed 650 rpm and IBC of 25 mm was 39.37. By the Taguchi method, when the factor levels for predictions of the design already exist in the experimental set, and corresponds to the run with the highest S/N ratio, which was the desired ratio, it would

suffice to seeing this as the optimum design (Ranjit, 1990). This experiment was run in triplicates for the Rushton impeller at 70°C, 600 rpm and 30 mm and at 60°C, 650 rpm and 25 mm for Elephant ear impeller respectively. Based on a 95% confidence level, the results were further analyzed by ANOVA to access the goodness of fit. The highest S/N ratio was at R^2 = 0.937 and 0.89 for the Rushton and Elephant ear impellers respectively.

Experimental results were fitted to a linear model, and the following equations were obtained (Equations 4 and5) where t, S and I are temperature, speed and IBC respectively:

$$Yield = 39.0624 - 0.0146t_{60} - 0.0604t_{65} - 0.0111S_{600} + 0.0509S_{650} - 0.1387I_{20} + 0.0578I_{25}$$
(4)

$$Yield = 39.06 - 0.13t_{60} - 0.12t_{65} - 0.29S_{600} + 0.07S_{650} - 0.27I_{20} + 0.21I_{25}$$
(5)

The statistical models obtained from the coded factor levels were only valid within the experimental range considered. The FAME yield (weight %) using the Rushton and Elephant impeller was obtained with respect to the temperature, speed and distance by Equations (4) and (5). This linear interaction is limited in expressing the system. The p-value (Table 6) showed that none of the factors had any significant effect on FAME yield. This statistical analysis would suffice for the present study if the time of peak yield was not considered. However, relating period of peak yield to FAME yield is important in considering the earlier stated objective that the reaction time affects product quality and quantity. Further analysis

Table 6. S/N ratio of yield.

Temperature (℃)	Speed (rpm)	IBC (mm)	FAME yield (%)(Rushton, unbaffled)	S/N ratio (yield)	FAME yield (%) (Elephant ear, baffled)	S/N ratio (yield)
60	600	20	87.719	38.86	91.73	39.25
60	650	25	91.16	39.20	**93.02**	39.37
60	700	30	90.01	39.09	91.45	39.22
65	600	25	89.59	39.05	91.5	39.23
65	650	30	90.133	39.10	91.54	39.23
65	700	20	87.73	38.86	89.17	39.00
70	600	30	**91.69**	39.25	90.27	39.11
70	650	20	89.60	39.05	91.02	39.18
70	700	25	90.36	39.12	92.39	39.31

was thus required with respect to the desired output that is yield and to accurately describe the WCO transesterification process. Figures 9 to 14 illustrate the interaction between the temperature, speed and IBC against yield time and yield using the Rushton impeller. The temperature, speed and IBC were respectively plotted against yield time and FAME yield. A smoothing regression technique using the weighted linear least square and a quadratic polynomial model for smoothing data were adopted to analyze the peak yield time with respect to temperature, speed and IBC (Table 7). The locally weighted regression using a weight function that down–weights data points by loess curve fitting function was performed on the data from the Rushton impeller.

Figures 9 to 14 show the surface plot of the interaction of the parameters with respect to FAME yield and yield time. The smoothed profile is shown as a surface curve and the original value for the different parameter as blue points. All values were judged to be significant based on this curve fit contained at a level of p = 0.05 with R^2 value between 0.93 to 0.96 which shows a good correlation using quadratic function. Based on loess fitting function, the correlation between FAME yield, peak time and temperature was high

(0.968) for all the data. The surface plot represented in Figures 9 and 14 illustrate the best operating conditions for obtaining maximum FAME yield and optimum yield time for the WCO transesterification with a FFA content of <2% weight. These operating conditions for maximum FAME yield and yield time were as follows:

Rushton impeller (unbaffled): 60 and 70°C at 700 rpm and 25 mm IBC at 5 to 15 min Elephant ear (baffled): 60°C, 700 rpm and 20 mm IBC at 10 min.

This non-parametric evaluation showed the interaction between the factors that were not obvious in the linear relationship established earlier. Yield time function in the work is considered as a necessary addition for parametric optimization.

Reaction time results

For impeller rotational speed (N) of 600, 650 and 700 rpm (10, 10.8, 11.7 s^{-1}), Reynolds number (Re = $\rho ND^2/\mu$), ranged up to 24590 to 29108 for the Rushton and 30189 to 35221 for the Elephant ear impeller. Typically, the reaction time would have been measured using conductivity,

thermocouple, or pH techniques (Paul et al., 2004), however, the pace of reaction and evolution of product was difficult to monitor and the time of FAME formation was used as the reaction time shown in Figures 5 to 8. Other methods such as PLIF and pH monitoring may not be adequate in estimating the reaction time to fit the transesterification model because of the cascade of reaction, liquid opacity and especially auto-catalysis which renders this measurement redundant. As it had been noted, the yield in this work was high and peak yield production was earlier (5 to 15 min of reaction time), hence estimation of the reaction time, especially at high turbulence would require more study.

FAME quality

The mean yield from the Taguchi design set the optimum level of FAME yield (91.70%) at 70°C, 600 rpm and 30 mm IBC for the Rushton while that for elephant ear was 60°C, 650 rpm and 25 mm. On the average, the DG and T level was twice as compared to ASTM standard for both Rushton (baffled and unbaffled) and the Elephant (baffled and unbaffled) reactors (Table 4), but MG,
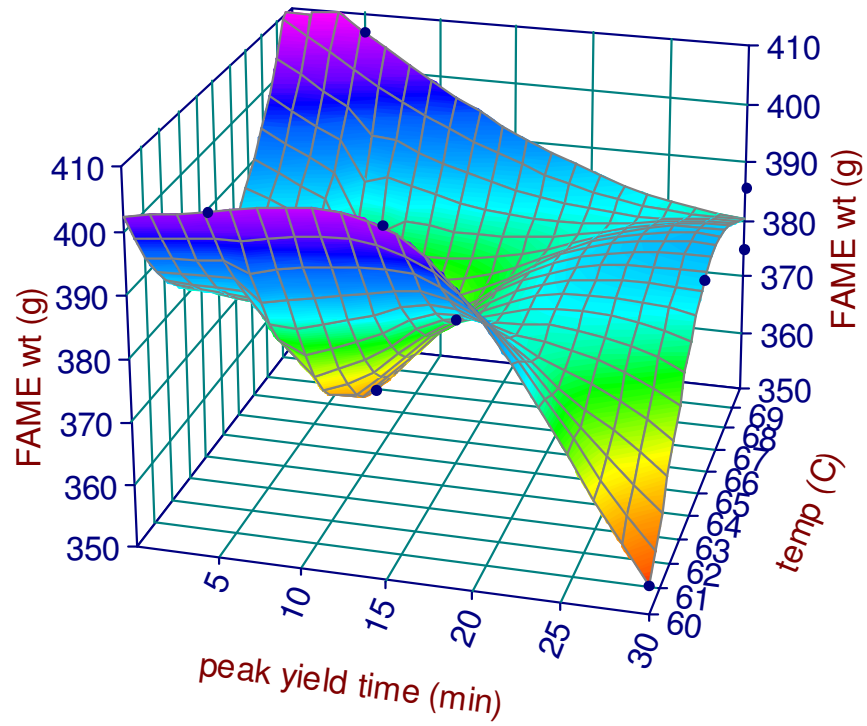
Figure 9. Response surface plot of FAME weight yield (410 g) as function of peak yield time (5 min) and temperature (68°C).
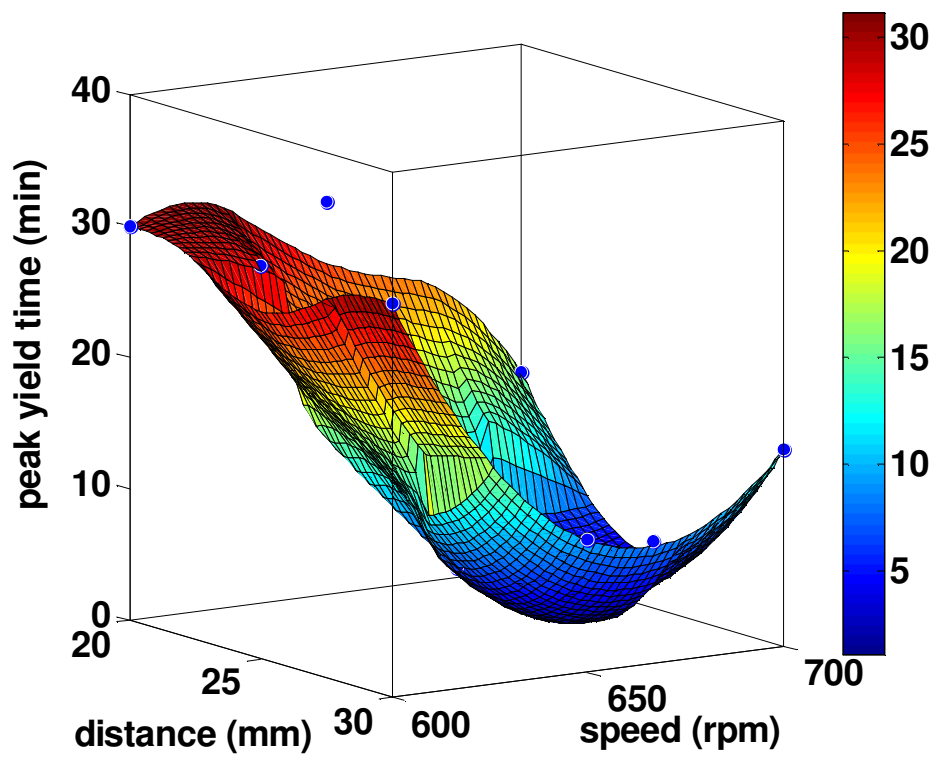
Figure 10. Response surface plot of FAME peak yield time (5 min) as a function of bottom impeller (25 to 30 mm) distance and speed (600 rpm).
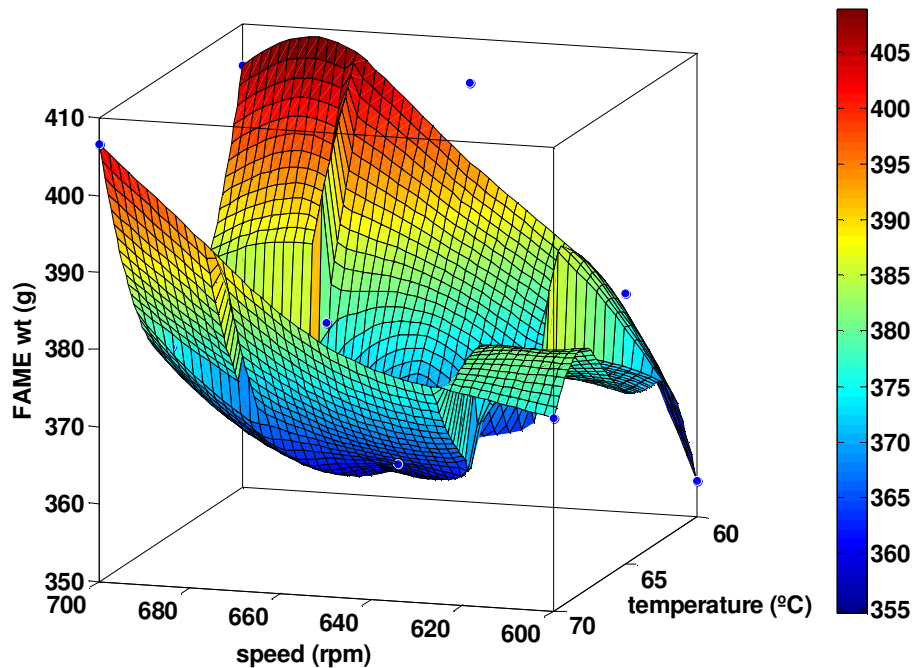
Figure 11. Response surface plot of FAME weight yield (410 g) as a function of temperature (70°C) and speed (700 rpm).
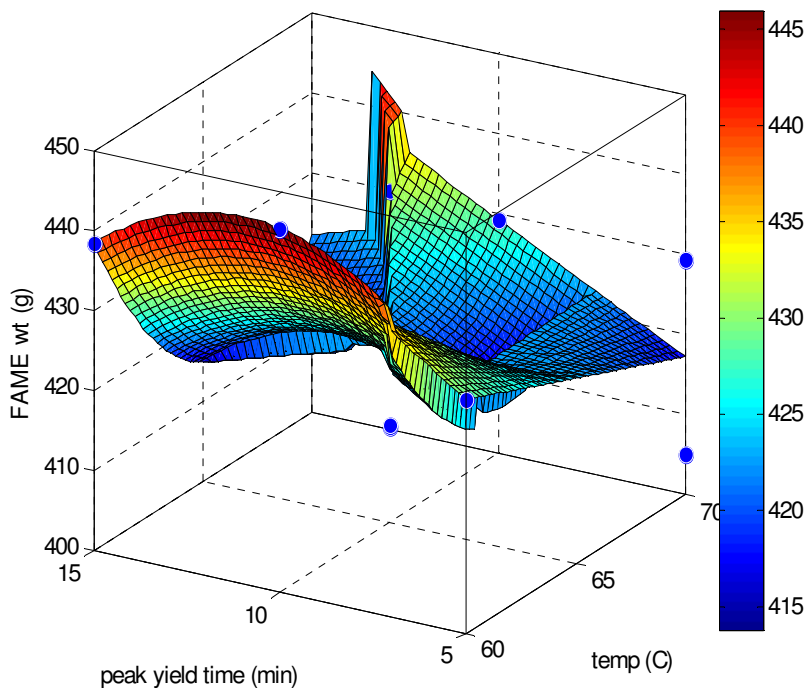
Figure 12. Response surface plot of FAME weight yield (438 g) as function of peak yield time (5 to 10 min) and temperature (60ºC).

G, TG content were within the range for the Elephant (baffled and unbaffled). However, the surface plot relieves that optimum FAME yield using the Rushton in unbaffled reactor could be obtained at the extreme of the
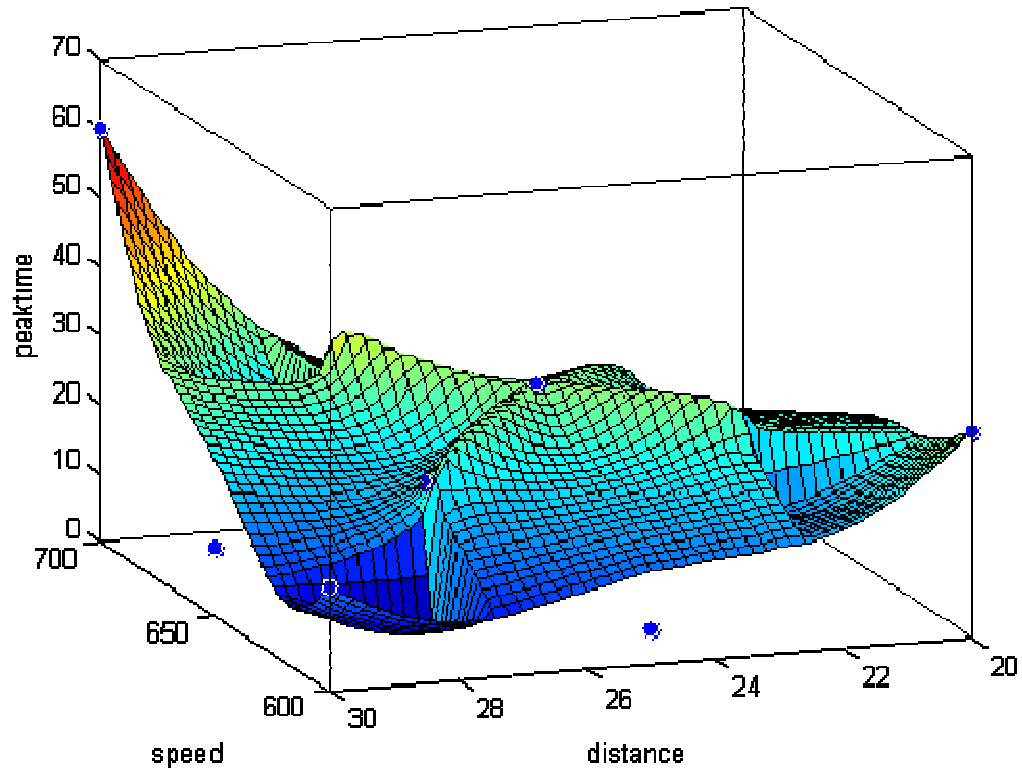
Figure 13. Response surface plot of FAME peak yield time (15 min) as a function of IBC (20 mm) distance and speed (600 rpm).
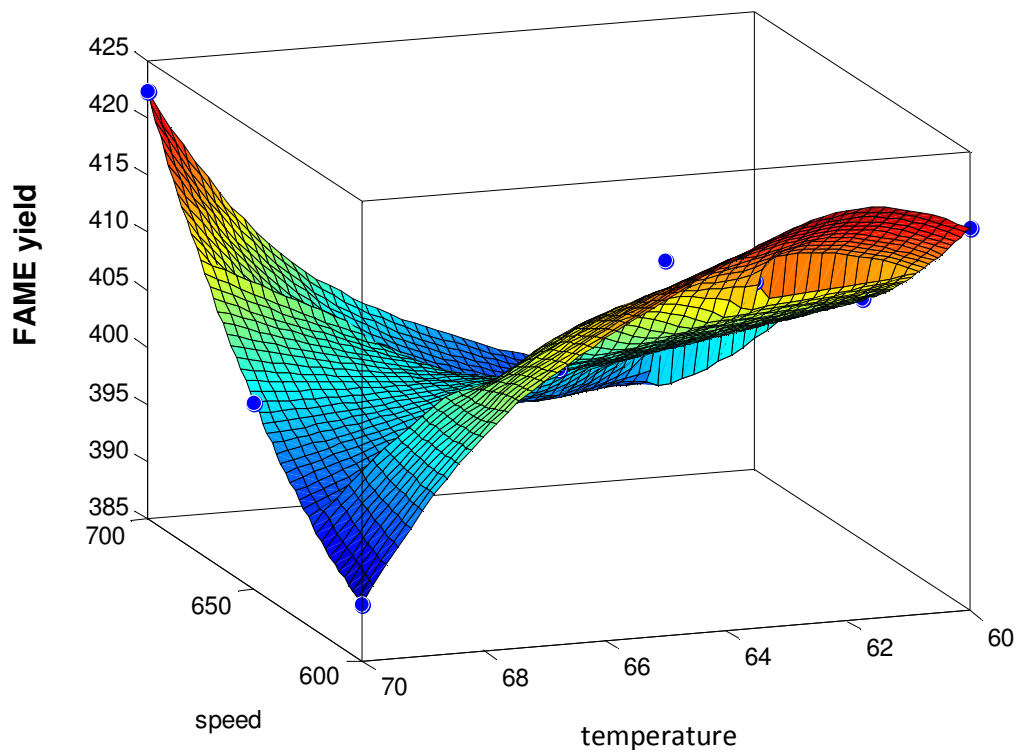
Figure 14. Response surface plot of FAME weight yield (438 g) as a function of temperature (60ºC) and speed (600 and 700 rpm).

Table 7. Statistical correlation of temperature; speed and IBC to yield and peak yield time.

Parameter	Rushton (peak yield time)			Elephant ear (peak yield time)		
	SE Coeff	T	p	SE Coeff	T	p
Constant	2.07	9.13	0.01	0.42	218.57	0
T	3.83	2.05	0.18	0.77	-0.57	0.63
S	3.83	-1.74	0.22	0.77	-0.72	0.55
ID	3.83	-2.74	0.11	0.77	1.34	0.31
T*S	5.74	-2.49	0.13	1.16	1.4	0.30
T*ID	5.74	0.87	0.48	1.16	-0.82	0.50
S*ID	5.74	1.87	0.20	1.16	-0.03	0.98

chosen speed that is 600 and 700 rpm and for Elephant ear 600 to 650 rpm within the range of other optimized parameter using the L_9 design. The result compliments earlier works on WCO optimization (Bautista et al., 2009), where the focus was extended to FAME purity and catalyst concentration which is encourages in view the fact that the a single step transesterification was used for the WCO transesterification and a recovery step was not added in this work. Further investigations are in progress to estimate the kinetics of the reaction in both configurations and optimize the performance of impeller which will be reported separately. As observed, changes in mixing produce obvious effects where the measured kinetics is limited not only by the rate of the reaction (Paul et al., 2004) but also by the rate of mixing. When also the kinetics of reaction changes as rates of reaction, mixing and mass transfer approach one another.

The outcome of this work showed that mixing affected transesterification process and thus the kinetics rate must reflect this based on the difference in the reactor configuration.

Conclusion

The Taguchi method based on the AO L_9 design was used to determine the effect of temperature, speed and IBC during mixing on the FAME yield from WCO transesterification along with peak yield/time factor, which had not been previously considered. The optimum reactor setting was found to be at 70°C, 650 rpm and IBC of 30 mm for a Rushton in unbaffled reactor and 60°C, speed 650 rpm and IBC of 25 mm for Elephant ear in baffled reactor. The improvement in the optimization using a surface response procedure extends the range for optimum yield and included period of peak yield. The S/N ratio ranked the impeller distance as having the highest impact on yield followed by temperature and speed for the unbaffled reactor using a Rushton impeller; and speed ranked highest followed by impeller distance and temperature in the baffled reactor using the Elephant ear impeller. Modification of experimentation particularly to optimize transesterification of WCO can significantly improve FAME yield with regards to reactor configuration to compliment previously investigated factors as this work showed that high yield was obtained using an Elephant ear impeller in a baffled reactor. Un-reacted T, DG and MG were other aspects which will elicit investigation with different configuration arrangement.

As the optimum yield time was between 5 to 30 min, the scale up ratio for industrial production would need to be determined and the subsequent step in this work is to use a CFD approach to model the mixing and further verify this result.

REFERENCES

Araujo VKWS, Hamacher S, Scavarda LF (2010). Economic assessment of biodiesel production from waste frying oils. Bioresour. Technol. 101(12): 4415-4422.

Baroutian S, Aroua MK, Raman AAA, Sulaiman NMN (2010). Potassium Hydroxide catalyst supported on palm shell activated carbon for transesterification of palm oil. Fuel Processing Technol. 91(11): 1378-1385

Bautista LF, Vicente G, Rodríguez R, Pacheco M (2009). Optimisation of FAME production from waste cooking oil for biodiesel use. Biomass Bioenergy, 33(5): 862-872.

Berrios M, Siles J, Martin M, Martin A (2007). A kinetic study of the esterification of free fatty acids (FFA) in sunflower oil. Fuel, 86(15): 2383-2388.

Canakci M (2007). The potential of restaurant waste lipids as biodiesel feedstocks. Bioresour. Technol. 98: 183-190.

Catharino RR, Haddad R, Cabrini LG, Cunha IBS, Sawaya ACHF, Eberlin MN (2005). Characterization of vegetable oils by electrospray ionization mass spectrometry fingerprinting: classification, quality, adulteration, and aging. Anal. Chem. 77(22): 7429-7433.

Chhetri AB, Watts KC, Islam MR (2008). Waste Cooking Oil as an Alternate Feedstock for Bodiesel Production. Energies, 1(1): 3-18.

Darnoko D, Cheryan M (2000). Kinetics of palm oil transesterification in a batch reactor. JAOCS. 77(12): 1263-1267.

de Sousa JS, Cavalcanti-Oliveira EA, Aranda DAG, Freire DMG (2010). Application of lipase from the physic nut (*Jatropha curcas* L.) to a new hybrid (enzyme/chemical) hydroesterification process for biodiesel production. J. Mol. Catalysis B: Enzymatic, 65(1-4): 133-137.

Demirbas A (2009) Political, economic and environmental impacts of biofuels: A review. Appl. Energy, 86: 108-117.

Ferella F, Mazziotti Di Celso G, De Michelis I, Stanisci V, Vegli F (2010). Optimization of the transesterification reaction in biodiesel production. Fuel, 89: 36-42.

Fernandes P (2010) Miniaturization in Biocatalysis. Int. J. Mol. Sci. 11(3): 858-879.

Freedman B, Butterfield RO, Pryde EH (1986). Transesterification

kinetics of soybean oil 1. J. Am. Oil Chem.' Society (JAOCS) 63(10): 1375-1380.

Gui M, Lee K, Bhatia S (2008). Feasibility of edible oil vs. non-edible oil vs. waste edible oil as biodiesel feedstock. Energy, 33(11): 1646-1653.

Issariyakul T, Kulkarni MG, Dalai AK, Bakhshi NN (2007). Production of biodiesel from waste fryer grease using mixed methanol/ethanol system. Fuel Proc. Technol. 88(5): 429-436.

Jena PC, Raheman H, Prasanna Kumar G, Machavaram R (2010). Biodiesel production from mixture of mahua and simarouba oils with high free fatty acids. Biomass Bioenergy, 34(8): 1108-1116.

Karmee SK, Chadha A (2005). Preparation of biodiesel from crude oil of *Pongamia pinnata*. Bioresource Tech. 96(13): 1425-1429.

Knothe G, Steidley KR (2009). A comparison of used cooking oils: A very heterogeneous feedstock for biodiesel. Bioresour. Technol. 100(23): 5796-5801.

Kulkarni MG, Dalai AK (2006). Waste Cooking Oil-An Economical Source for Biodiesel: A Review. Ind. Eng. Chem. Res. 45(9): 2901-2913.

Ma F, Clements LD, Hanna MA (1998). Biodiesel fuel from animal fat. Ancillary studies on transesterification of beef tallow. Ind. Eng. Chem. Res. 37(9): 3768-3771.

May CY (2004). Transesterification of palm oil: effect of reaction parameters. J. Oil Palm Res. 16(2): 1-11.

McCurry JD, Wang CX, Zone WFT (2007). Analysis of glycerin and glycerides in biodiesel (B100) using ASTM D6584 and EN14105, Agilent Application Note Publication.

Meher L, Naik S, Das L (2004). Methanolysis of *Pongamia pinnata* (karanja) oil for production of biodiesel. J. Sci. Ind. Res. 63: 913-918.

Meher L, Vidya Sagar D, Naik S (2006). Technical aspects of biodiesel production by transesterification-a review. Renewable Sustain. Energy Rev., 10(3): 248-268.

Mittelbach M, Schober S (2003). The influence of antioxidants on the oxidation stability of biodiesel. J. Am. Oil Chem.' Society 80(8): 817-823.

Noureddini H, D Zhu (1997). Kinetics of transesterification of soybean oil. J. Am. Oil Chem.' Society 74(11): 1457-1463.

Paul EL, Atiemo-Obeng VA, Kresta SM (2004). Handbook of industrial mixing Wiley Online Library.

Ramos MJ, Fernandez CM Casas A, Rodriguez L, Perez A (2009). Influence of fatty acid composition of raw materials on biodiesel properties. Bioresour. Technol. 100(1): 261-268.

Ranjit R (1990). A primer on the Taguchi method van Nostrand Reinhold.

Sharma Y, Singh B, Upadhyay S (2008). Advancements in development and characterization of biodiesel: A review. Fuel, 87(12): 2355-2373.

Stamenkovic OS, Lazic M, Todorovic Z, Veljkovic V, Skala D (2007). The effect of agitation intensity on alkali-catalyzed methanolysis of sunflower oil. Bioresour. Technol. 98(14): 2688-2699.

Szalai ES, Kukura J, Arratia PE, Muzzio FJ (2003). Effect of hydrodynamics on reactive mixing in laminar flows. Am. Institute of Chem. Engineers J. 49(1): 168-179.

Valle P, Velez A, Hegel P, Mabe G, Brignole E (2010). Biodiesel production using supercritical alcohols with a non-edible vegetable oil in a batch reactor. J. Supercritical Fluids, 54(1): 61-70.

Vicente G, Martinez M, Aracil J (2004). Integrated biodiesel production: a comparison of different homogeneous catalysts systems. Bioresour. Technol. 92(3): 297-305.

Yang Y, Yoon RH, Telionis DP, Weber A, Foreman D (2008). Flow Property Measurements of Stirred-Tank Flow across Three Reynolds Number Decades. ASME Conference Proceedings, pp. 329-336.

Zhang Y, Dube M, McLean D, Kates M (2003). Biodiesel production from waste cooking oil: 1. Process design and technological assessment. Bioresour. Technol. 89(1): 1-16.

Zhou W, Boocock DGB (2006). Phase distributions of alcohol, glycerol, and catalyst in the transesterification of soybean oil. J. Am. Oil Chem.' Society. 83(12): 1047-1052.